

WAKE ANALYSIS FROM THE FIRST PRINCIPLES OF HYDRODYNAMICS

P.K.Sarma*, Y.V.V.S.N.Murty*, Rajesh Ghosh*, M.TimmaRaju*, Y.Radhika*
RajeswaraReddy*, C.P.Ramnarayanan °

*GITAM University, Visakhapatnam-45, INDIA
°GTRE, Bangalore

ABSTRACT

The theoretical approach presents the dynamics of the wake under ideal conditions free from cavitations and boundary layer separation effects in the stern region during cruise of a ship. Principles of conservation of momentum and kinetic energy are considered in the formulation. The power rating of the propeller is found to be the dominant parameter determining the active length of the wake for the range $2 \times 10^6 \text{ W} < \text{POWER} < 15 \times 10^6 \text{ W}$. However, the profile of the wake is uniquely considered independent of the power of the propeller. The assumption such as a logarithmic variation of the profile of the wake can be altered by any of the suitable functional relationship depending on aerial observations and the data.

1. INTRODUCTION

The wake behind a ship is a region that consists of complex hydrodynamic flow phenomenon characterized by temporally and spatially varying flow conditions like local fluid velocity, pressure, turbulent kinetic energy and dissipation etc. Originally the wake model was only based on air entrapping sources near each of the propellers and the ship hull. The physical mechanism of ship wake is due to the turbulence generated by the movement of the ship. This wake develops and grows in time and characterizes the scale of turbulence. Ship wake Properties depend on the size, the speed and the propulsion system of the ship. The wake created by rotating propeller resembles a rotating column of water having both linear and angular momentum. This column of water slowly broadens since the water surrounding this column entrains due to the eddy diffusion. Near to the propeller the wake is controlled by angular momentum but for astern the wake is controlled by linear momentum neglecting free surface effects [1]. The thrust provided by the propeller can be related to the rate of production of linear momentum (Newton's second law), P^* . In the far wake, observations indicate that the mean velocity profile is close to Gaussian [2]. Evolution of a wake with both linear and angular momentum involves eddy creation and diffusion from both types of velocity shear. The relation between the wake width, b , and the distance astern, z , for the combined wake is given by James K.E. Tunaley [3]. Actuator disc model is used to estimate the rates of production of linear and angular momentum together with experimental observations on stock propellers in open water. The engine power of the ship is estimated by calculating the resistance force to the motion by simulating the flow around the ship. Navier-Stokes equation was solved computationally using the finite volume method for simulating the flow around the hull to estimate the engine power [4]. The work done by the torque

at the propeller is equal to the work done by the thrust in opposing the drag along with the kinetic energy of the water gained during its acceleration and its rotation as it passes through the propeller. The translational and angular velocities in the propeller race some distance aft of the propeller can be estimated in terms of the propeller slip ratio, σ , and the propeller efficiency ' η ' effectively by Comstock [5] as $a^1 = 1 - \eta \cdot (1 + \sigma/2)$ where a^1 is the fraction of the power at the propeller converted into rotation of the fluid. The variation of velocities also changes with respect to the propeller depth and the distance astern of the ship. When the propeller depth is set at 6mtrs reveals that the velocities first increase with distance astern and then decrease. They are also generally reduced as the screw depth is increased. Bubble concentration is also used to model the ship and propeller and it was found that bubble concentration is a function of time [6]. Geometric model of ship wake was predicted by Liu Chunwu, using particle theory for analyzing the ship wake bubble dynamics. The model is simplified by considering viscous resistance of water such that the viscous resistance F_a suffered by diffusing particle given by $F_a = 0.5 \Pi R^2 \rho_1 C_v^2 D$ [7]. Ship wake bubble dynamics was studied by developing geometrical model based on the particle system theory and bubble particle kinetics equations. Initial position of the particle is taken as the position of the ship and particles generates, astern of the ship. Wake flow geometry model is developed by solving the acceleration, velocity and position of the bubble particle. The problems associated with traditional methods like distortion of ship wake geometric model, including inflexion point and gap are solved in this method [8]. Dispersion Wake field model based on buoyancy, dissolution and air volume ratio was studied by SveinVagle [9] and found that wakes decay exponentially with an e-folding time between 40 and

60secs. The wake characteristics are found to depend on the Reynolds number, Re which is dimensionless and represents the ratio of inertial forces to viscous forces. It is given by $Re = UL/v$, where U is the flow velocity, L is a characteristic length, such as the length or diameter of the obstacle and v is the kinematic viscosity. The Reynolds number in a wake immediately aft of a ship of length 100 m traveling at 10 m/s in water with a kinematic viscosity of about $10^{-6} \text{ m}^2/\text{s}$ is about 10^9 . For higher Reynolds number viscosity can be ignored. Within the wake itself, it is appropriate to define another Reynolds number involving the wake diameter and the flow mean velocity relative to the ocean; this decreases with distance astern from a typical value of 10^8 [10]. Kelvin's wake consists of a system of ripples occurring inside a cone of 39 degrees originating at the ship's bow. The turbulent wake's width W depends upon ship dimensions, more specifically its beam (width) B , and its length L the wake width at a distance r is given by $W(r) = 1.9 B^{4/5} r^{1/5}$ [11]. The wake length is a more difficult problem and depends upon sea state. The turbulent wake is caused by water displacement due to the ship's hull and propulsion system. This water displacement has a kinetic energy decreasing according to $r^{-4/5}$ [12]. The flow in the wake is extremely complex, being a superposition (often non-linear) of turbulent shear flows, coherent vortex flows, free surface waves, bubble flows and potentially internal waves. One of the most observable features in the wake of a surface ship is the long, narrow region of relatively calm water that extends aft of the ship. This "dead water" or Center line wake region is typically two to four ship beams in width and, depending on the sea state and the ship speed, persists for upwards of many tens of ship lengths aft. The near-field centerline surface wake is a composite of the various contributions from the individual flows above and interactions between them [13]. Numerical study of two-dimensional steady, incompressible MHD flow past a circular cylinder in cylindrical and polar co-ordinates reveals that vortices are formed in the flow field with increase in Reynolds number [14]. Surface Lagrangian velocity profiles in the near viscous wake region of a high speed twin screw vessel is studied by [15]. Downstream rate of decay of both the mean longitudinal and transverse velocity components. The spatial rates of decay of these surface velocity signatures were fit to a general expression of the form $W_i = a(X/L)^b$ where W_i is the corresponding wake fraction in the x and y directions, respectively, L is the ship length and a and b are regression coefficients.

2. FORMULATION OF THE MODEL

The propeller as shown in figure 1 creates an out flow away from the stern of the ship and the flow rate depends on the power transmitted by the shaft. The wake is generated at the stern and the velocity profiles gradually degenerate with substantial loss in momentum and Kinetic energy. The magnitude of the central velocity along the axis of the stream tube also reduces to local disturbances.

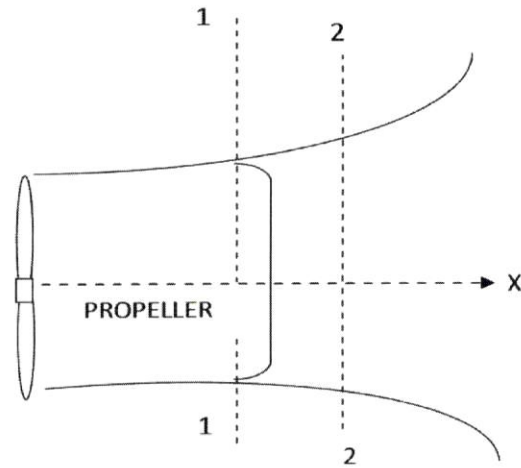


Figure 1. Steam tube generated by the propeller. An element of the wake between sections 1-1 and 2-2 shown in the Figure 2 is considered

The analysis is performed in two ways

- Application of Conservation of momentum
- Application of Conservation of energy

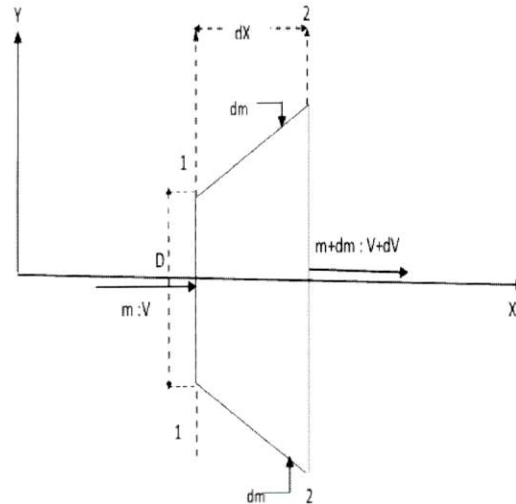


Figure 2. Differential element of the wake

2.1 Momentum dissipation model (M.D.M)

Applying conservation of momentum for the element of the developing wake between sections 1-1 and 2-2 of Fig (1) Viz., the rate of change in momentum is equal to the external opposing force of the ambient medium to the developing wake in ambient medium it follows

$$\frac{d[MV]}{dX} + V \frac{dM}{dX} = -\tau\pi D$$

Where m is the mass flow (1)

V is the average flow velocity

X is the spatial distance measured from the stern of the ship

Defining the following

$$Re = \frac{4m}{\pi D \mu} = \frac{VD}{\vartheta} \quad (2)$$

$$\tau = \frac{1}{2} f \rho V^2 \quad (3)$$

'f' is the friction coefficient an unknown magnitude and introducing equations (2) and (3) into equation (1) the following dimensionless equation can be arrived at

$$3 \frac{dRe}{d\xi} = -2f \frac{Re}{D^+} - \frac{Re}{D^+} \frac{dD^+}{d\xi} \quad (4)$$

Where

$$\xi = \left[\frac{X}{D_0} \right] : D^+(\xi) = \left[\frac{D(X)}{D_0} \right] \quad (5)$$

D₀ is the diameter of the propeller.

Equation (4) consists of two dependent variables Re(ξ) & D⁺(ξ) which are strongly dependent on the spatial variable (ξ). The solution of equation (5) requires a hypothesis or a naval architecture data documented from practical considerations.

2.2 Kinetic energy Dissipation model (K.D.M)

The propeller is the driving element to maintain cruise of the ship. The speed of the ship is closely related to the power transmitted by the shaft inducing out flow of water in a direction opposite to the motion of the ship. The wake length depends on the gradual dissipation of kinetic energy by doing work against the relatively stationary ambience of waters. In other words the dynamics of the submerged jet created by the shaft determines the zone of the wake. Thus, the rate of dissipation of kinetic energy = Work done against stationary ambient medium

Thus, for the element 1-1, 2-2 shown in figure (1)

$$\frac{d}{dX} [mV^2] = -\tau V \pi D \quad (6)$$

Equation (6) in dimensionless form can be manipulated as follows

$$\frac{d(Re)}{d\xi} = \frac{Re}{3} \left[\frac{1}{D^+} \frac{dD^+}{d\xi} - \frac{2f}{D^+} \right] \quad (7)$$

It can be seen that the differential equations (4) and (7) are not the same in either case to yield identical results. However, the trends of variations of the wake parameters must be same. Equations (4) and (7) contain two dependent variables Re; D⁺ which are functions of independent variable ξ. To obtain independent solutions it is essential to consider one of the dependent parameters Re or D⁺ is a known function of ξ. Thus, two approaches are thought of in presenting the results which are to be subsequently corrected with the practical observations from the wake during cruise.

Method 1: D⁺ is assumed to be a function of ξ, and Variation of Re with respect to the spatial variable ξ, can be

obtained from the differential equations (4) and (7). Several functional relationships for D⁺ can be assumed as a function of ξ. The best choice of course, depends on practical considerations.

$$D^+ = 1 + B \left[\frac{X}{D_0} \right] \quad (8)$$

D⁺ is a linear function of ξ. B represents the slope of the linear function

$$D^+ = \left\{ 1 + B \left[\frac{X}{D_0} \right] \right\}^m \quad (9)$$

D⁺ is a power law variation with respect to ξ with a variable unknown exponent 'm'

$$D^+ = B \left\{ 1 + \ln \left[1 + \frac{X}{D_0} \right] \right\} \quad (10)$$

D⁺ is a logarithmic function of ξ. Magnitude of B depends on the impact of boundary layer separation at the stern and other secondary vortices effects on the diameter of the stream tube generated by the propeller

$$D^+ = \left\{ 1 + B \ln \left[1 + \frac{X}{D_0} \right] \right\}^m \quad (11)$$

Introduction of the exponent m makes the relationship more general to account for variable propeller, power. The best choice or alternatives depend on the aerial observations of the wake. Some typical results can be obtained by making use of some equations from the group of equations (8) to (11). For example choice of Equation (8) yields exact solution. Typical results for both momentum dissipation model and kinetic energy model are presented choosing equation (10) only with the magnitude of B tentatively chosen as unity. However, the choice of magnitude of B depends on practical considerations.

Numerical solution of equations (4) and (7): respectively in finite difference form are presented as follows:

$$RE(I+1) = RE(I) - \frac{0.66 * DZ * F * RE(I)}{1 + ALOG(1 + Z(I))} - \frac{0.33 * RE(I) * (1 + Z(I))}{1 + ALOG(1 + Z(I))} \quad (12)$$

$$RE(I + 1) = RE(I)$$

$$-DZ \left[\frac{1}{\frac{[1 + A \log(1 + Z(I))] * [1 + Z(I)]}{2 * F} - \frac{1}{1 + A \log(1 + Z(I))}} \right]$$

(13)

Where $Z(I) = DZ * (I-1)$, DZ is spatial step size, I is the variable node and $1 < I < J$, J is the node final where $RE(J) = 2000$. F is the friction coefficient to be obtained by iterative procedure such that $RE(J) = 2000$ at $Z(J)$ at a prescribed wake length S measured from the propeller. For the case of turbulent submerged jets F can also be a modification of Blasius equation defined as $F = C[0.046/RE(I)^{0.2}]$ where $C = F[\text{Power Of The Propeller}]$, or $F = \text{constant} [RE(I)]^m$.

Thus, the two models are programmed and results are presented from the flow dynamic study developed. The salient results are presented in Tables 1 & 2. It can be seen that as the propeller power increases (see columns 3 & 4) the input Reynolds number increases. Further, the length of the wake also increases. It must be noted that for the models as per the assumptions adopted in the formulation the wake profile would remain the same except the wake length X (column 2) which is strongly dependent on the power. The nature of wake profiles employed in the analysis are shown in figure (3) of equation (3). In addition the average friction coefficient F for a given power varying with $Re(1)$ is shown plotted in fig 4 for model 1&2. The magnitudes deviate though the orders are the same. In figure(4) the variation of local Reynolds with the distance measured in meters from the stern of the ship is found to be decreasing till the flow of wake waters decreases substantially. In the analysis $RE(J) = 2000$ is fixed as the limit in obtaining $X(J)$ in the program. Figures (5) and (6) respectively depict the results from the momentum and kinetic energy dissipation models.

Method 2:

Considering $Re = F [Re(\zeta)]$ as a known variable the wake profile can be solved i.e. $D^+ = F[D^+(\zeta)]$

Thus, for an exponential variation it can be assumed

$$\frac{Re(\xi)}{Re(\xi = 0)} = \text{Exp}[-\beta \xi]$$

$$\text{where } \beta = -\frac{1}{\xi_L} \ln \left[\frac{Re(\xi_L)}{Re(\xi = 0)} \right] \quad (14)$$

Substituting equation (14) in equation (4) the differential equation $D^+ = D^+(\xi)$ is as follows:

$$\frac{1}{D^+} \frac{dD^+}{d\xi} + \frac{2f}{D^+} = 3\beta \quad (15)$$

The boundary condition to solve equation (15) is that at $\xi = 0$, $D^+ = D^+(\xi = 0)$

(16)

Typical results from equations (14), (16) are presented in the salient results from equations (14), (15) and (16) are shown in table 3. Besides the results are represented in Figures (8)-(12).

Table 1. Salient runs for kinetic energy model for different powers.

F	X	Power	RE (-1)	R	-R
0.4395	503.1	2.00E+06	2.44E+07	9.19	-9.192
0.4118	556.2	3.00E+06	2.79E+07	9.34	-9.342
0.3868	609.3	4.00E+06	3.07E+07	9.47	-9.478
0.3645	662.4	5.00E+06	3.31E+07	9.60	-9.603
0.3446	716.4	6.00E+06	3.52E+07	9.72	-9.72
0.3247	775.8	7.00E+06	3.70E+07	9.83	-9.839
0.3096	828.0	8.00E+06	3.87E+07	9.93	-9.936
0.2958	880.2	9.00E+06	4.03E+07	10.0	-10.02
0.2831	934.2	1.00E+07	4.17E+07	10.1	-10.11
0.2716	986.4	1.10E+07	4.30E+07	10.1	-10.19
0.2611	1039.	1.20E+07	4.43E+07	10.2	-10.27
0.2512	1093.	1.30E+07	4.55E+07	10.3	-10.35
0.2422	1146.	1.40E+07	4.66E+07	10.4	-10.42
0.2322	1211.	1.50E+07	4.77E+07	10.5	-10.50
0.2249	1262.	1.60E+07	4.88E+07	10.5	-10.56

Table 2. Salient runs for momentum dissipation model for different powers

F	X	Power	RE(1)	R	-R
0.373	500.4	2.00E+06	2.43E+07	9.18	-9.184
0.350	554.4	3.00E+06	2.79E+07	9.33	-9.337
0.329	607.5	4.00E+06	3.07E+07	9.47	-9.473
0.309	666.0	5.00E+06	3.31E+07	9.61	-9.611
0.292	719.1	6.00E+06	3.51E+07	9.72	-9.725
0.278	771.3	7.00E+06	3.70E+07	9.83	-9.83
0.265	824.4	8.00E+06	3.87E+07	9.93	-9.93
0.253	877.5	9.00E+06	4.02E+07	10.0	-10.02
0.242	931.5	1.00E+07	4.16E+07	10.1	-10.11
0.230	993.6	1.10E+07	4.30E+07	10.2	-10.20
0.222	1045.0	1.20E+07	4.40E+07	10.2	-10.28
0.214	1097.1	1.30E+07	4.50E+07	10.3	-10.35
0.206	1150.2	1.40E+07	4.20E+07	10.4	-10.42
0.199	1203.3	1.50E+07	4.34E+07	10.4	-10.49
0.193	1256.4	1.60E+07	4.87E+07	10.5	-10.56

Table 3. Typical Results from Equ.(14) & (15)

POWER	X	RE(I)	R	-R	F
1.00E+06	500.0	1.60E+07	10.00	-10.00	0.5183
2.00E+06	571.429	2.10E+07	12.14	-12.14	0.5654
3.00E+06	642.857	2.40E+07	14.28	-14.28	0.6002
4.00E+06	714.286	2.60E+07	16.42	-16.42	0.6279
5.00E+06	785.714	2.80E+07	18.57	-18.57	0.6505
6.00E+06	857.143	3.00E+07	20.71	-20.71	0.6695
7.00E+06	928.571	3.20E+07	22.85	-22.85	0.6857
8.00E+06	1000.00	3.30E+07	25.00	-25.00	0.6998
9.00E+06	1071.42	3.50E+07	27.14	-27.14	0.7121
1.00E+07	1142.85	3.60E+07	29.28	-29.28	0.7230
1.10E+07	1214.28	3.70E+07	31.42	-31.42	0.7327
1.20E+07	1285.71	3.80E+07	33.57	-33.57	0.7415
1.30E+07	1357.14	3.90E+07	35.71	-35.71	0.7494
1.40E+07	1428.57	4.00E+07	37.85	-37.85	0.7566
1.50E+07	1500.00	4.10E+07	40.00	-40.00	0.7632
1.60E+07	1571.42	4.20E+07	42.14	-42.14	0.7692
1.70E+07	1642.85	4.30E+07	44.28	-44.28	0.7748
1.80E+07	1714.28	4.40E+07	46.42	-46.42	0.7800
1.90E+07	1785.71	4.50E+07	48.57	-48.57	0.7849
2.00E+07	1857.14	4.50E+07	50.71	-50.71	0.7894

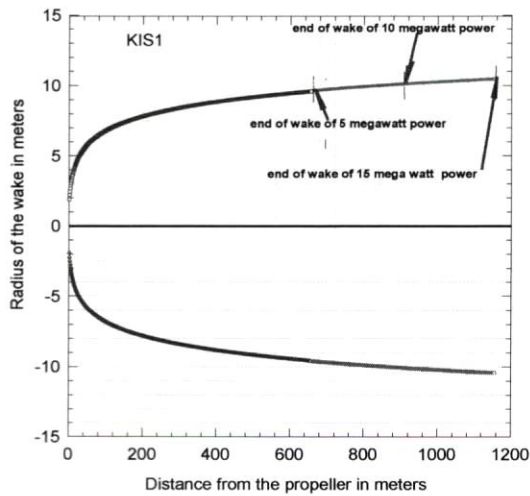


Figure3. Wake profiles for different powers

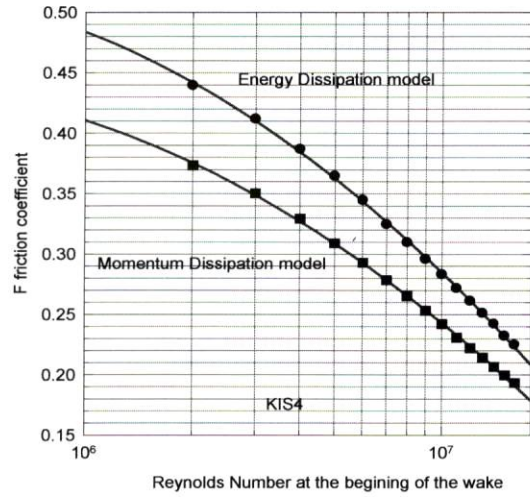


Figure 4. Variation of friction coefficient with RE(I)

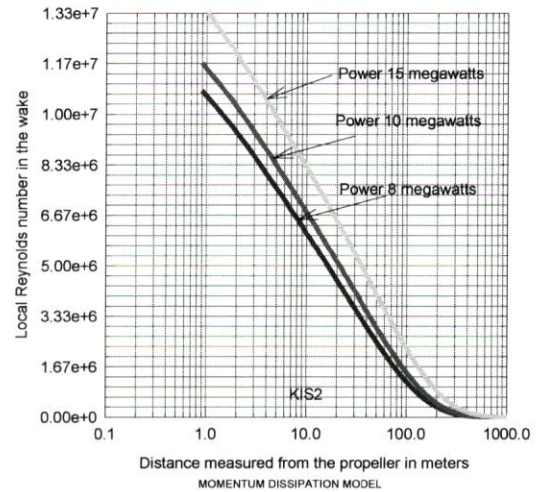


Figure5. Local variation of Re with X in momentum dissipation model

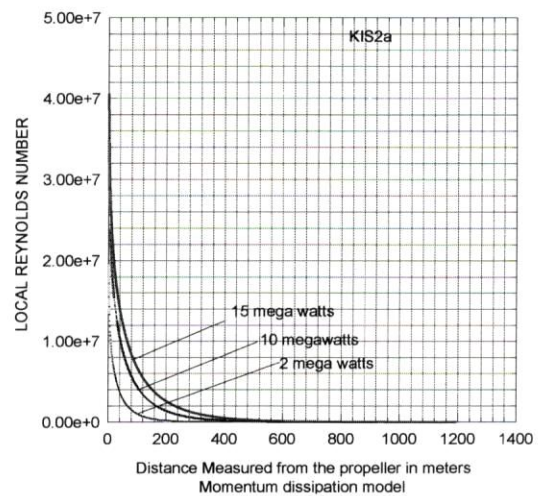


Figure6. Local variation of Re with X in Momentum dissipation model

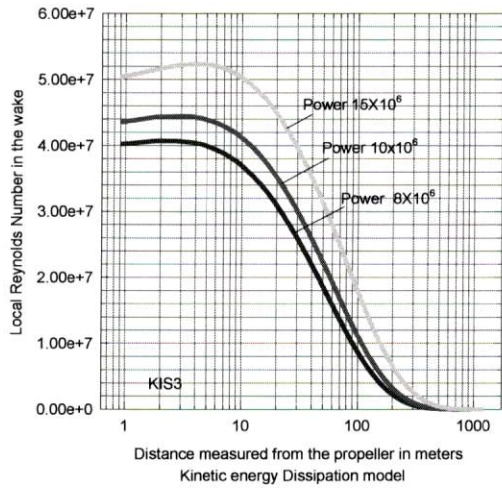


Figure7. Local variation of Re with X in kinetic energy dissipation model

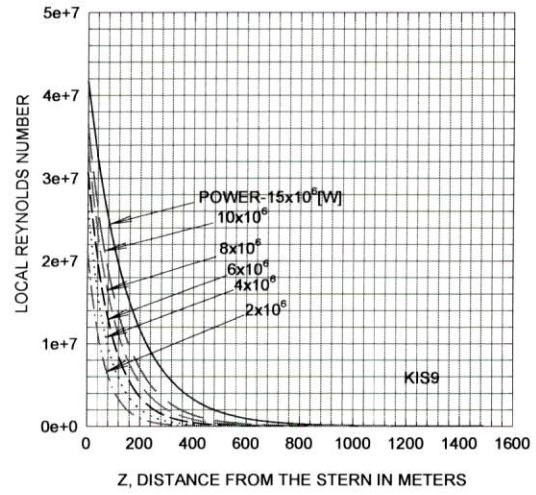


Figure10. Variation of local wake Re with power

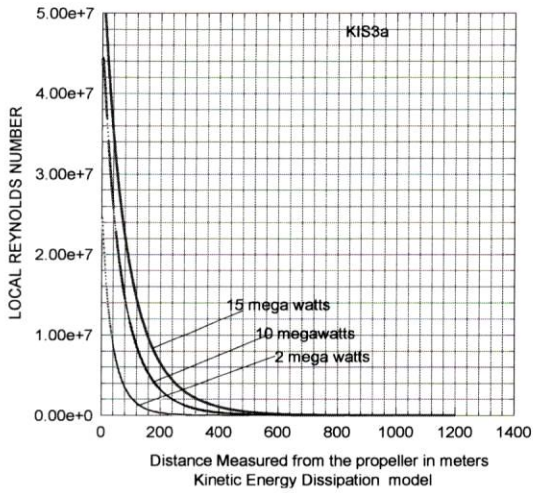


Figure8. Local variation of Re with X in kinetic energy dissipation model

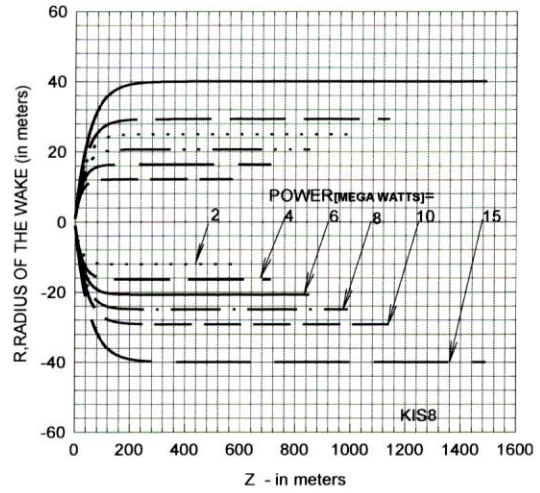


Figure11. Variation of wake profile with power

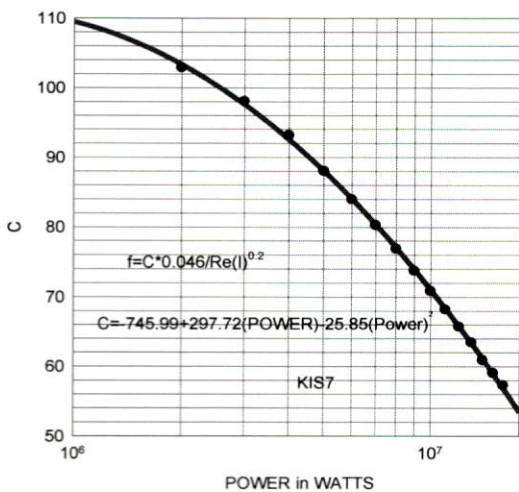


Figure9. Modification of Blasius equation for submerged jets

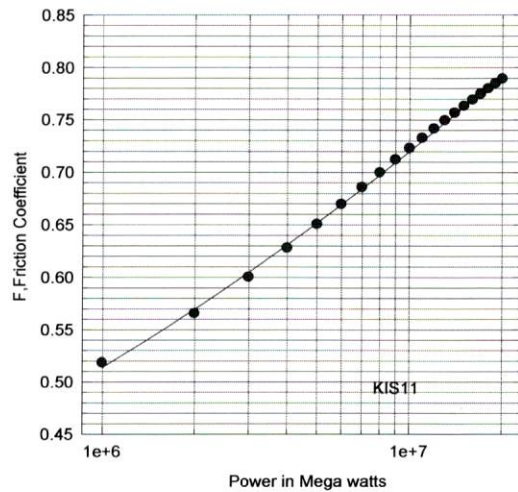


Figure12. Variation of friction coefficient with power

3. CONCLUSIONS

The analysis offers results for an ideal case of wake without cavitations and air entrainment effects in the turbulent wake in the stern region. The two phase wake formation is associated with cruise and navigational effects generating boundary layer separation in the hull region of the vessel.

4. REFERENCES

1. James K.E. Tunaley, Ship's Turbulent Propeller Wake: Combined Swirling and Linear Momentum Wake "London research and development corporation December 31st 2010
2. A.I. Serviente and V.C. Patel, Experiments in the Turbulent Near Wake of an Axisymmetric Body, AIAA Journal, vol. 37(12), pp 1670-1773, 1999
3. James K.E. Tunaley, Ship's Turbulent Propeller Wake: Combined Swirling and Linear Momentum Wake. December 31st 2010. J.K.E. Tunaley is with London Research and Development Corporation.
4. C. Biserni, M. De Luca, E.Lorenzini, C.Ragazzini, Theoretical and numerical investigation on ship motion and propulsion in Marine Engg. International journal of heat and technology. Vol28, No2, pp5-9, 2010.
5. J.P. Comstock (ed.), Principles of Naval Architecture, SNAME, N.Y., 1967
6. A.Sutin, Acoustic measurement of bubbles in the wake of a ship model in a tank. Acoustic 08 Paris June29-july 4,2008
7. Liu Chunwu, Li Ting, Huang Zhiping, Zhao Dexin, Zhang Yimeng, Ship Wake Simulation Based on Particle System in Virtual Test. Proceedings of the World Congress on Engineering 2011 Vol. IWCE 2011, July 6 - 8, 2011, London, U.K
8. Liu Chunwu, Li Ting, Huang Zhiping, Zhao Dexin, Zhang Yimeng, Ship Wake Simulation Based on Particle System in Virtual Test. Proceedings of the World Congress on Engineering 2011 Vol I WCE 2011, July 6 - 8, 2011, London, U.K.
9. SveinVagle, Acoustic measurements of the sound-speed profile in the bubbly wake formed by a small motor boat. J. Acoust. Soc. Am. 117 (1), January 2005.
10. James K. E. Tunaley, Theory of the Turbulent Far-Wake. LRDC 2011-01-31-001 January 31st, 2011.
11. G. Zilman, A. Zapolski, and M. Marom, The speed and beam of a ship from its wake's SAR images. IEEE Transactions on Geoscience and Remote Sensing, vol. 42, no. 10, pp. 2335-2343, 2004.
12. A. Benilov, G. Bang, A. Safray, and I. Tkachenko, Shipwake detectability in the ocean turbulent environment. Proceedings of the 23rd Symposium on Naval Hydrodynamics, pp. 687-703, 2001.
13. Reed, A.M., Beck, R.F., Grivwn, O.M. And Peh'zer, Hydrodynamics of remotely sensed surface ship wakes. SNAME Trans. 98, 319-363.
14. V. Ambethkar, Numerical study of MHD flow past a circular cylinder at high Reynolds number. International journal of heat and technology. Vol. 27, No. 1, pp. 111-116, 2009.
15. L. Meadows, Lagrangian velocity profiles in the wake of a high speed vessel. Ocean Engg, Vol. 21, No 2, pp. 221-242, 1994

5. NOMENCLATURE

D	Diameter of Wake
f	Friction Co-efficient
m	Mass of the fluid
P	Power in Megawatts'
V	Velocity of the fluid
Re	Reynolds number
X ⁺	Dimensionless distance astern of the ship
Z	Number of Iterations

Greek symbol

τ	Shear stress
μ	Dynamic viscosity, Ns/m ²
ν	Kinematic viscosity, m ² /s
ρ	Density of the fluid, kg/m ³

